SASI in Black Hole Accretions

Shoichi Yamada (Waseda Univ.)
Hiroki Nagakura (Waseda Univ.)

SN workshop @ IHP July 2 2008

Outline

General relativistic linear and nonlinear analysis of non-axisymmetric SASI in equatorial accretions to non-rotating and rotating black holes

1. Introduction
2. Unperturbed steady accretion flows with a standing shock wave
3. Linear Analysis
4. Numerical simulations of nonlinear evolutions of SASI
5. Astrophysical Implications
6. Summary

1. Introduction

Motivations of this work:

1. **To better understand the physics of SASI in broader perspectives.**
   — Standing shock waves can exist in black hole accretions and have instabilities similar to those in neutron star accretions
2. **to study the nature of black hole accretions.**
   — Black hole accretions will occur not only for binaries but also for collapses of very massive stars
   — GRBs for rapid rotators and failed SNe for slow rotators?
3. **to find possible astrophysical implications.**
   — Black hole accretions are known to show various temporal variations.

Previous works:

- **The existence of standing shocks in black hole accretions:**
  - **Fukue, 1987, PASJ 39, 309**: general relativistic, conical thin disk around Schwarzschild BHs, adiabatic, inviscid
  - **Chakrabarti, MNRAS 1989, 240, 7**: pseudo Newtonian, isothermal slab thin disk
- **The stability against axisymmetric perturbations:**
  - **Nakayama, MNRAS 1994, 270, 871, MNRAS 1996, 281, 226**: Newtonian and general relativistic, slab and conical thin disks
  - **Chakrabarti & Molteni, ApJ 1993, 417, 671**: 1D pseudo Newtonian simulations
  - **Nobuta & Hanawa, 1994, PASJ 46, 257**: pseudo Newtonian linear analysis and numerical simulations, isothermal slab thin disks
  - **Okuda et al., 2007, MNRAS 377, 1431**: 2D axisymmetric , pseudo Newtonian simulations, inviscid but with radiation transport
- **stability against non-axisymmetric perturbations:**
  - **Molteni et al., 1999, ApJ 516, 411**: 2D pseudo Newtonian simulations in slab thin disks, invscid
  - **Foglizzo, 2002, A&A 392, 353**: linear analysis of isothermal Bondi accretion with a shock
  - **Gu & Foglizzo, 2003, A&A 409, 1, Gu & Lu, 2006, MNRAS 365, 647**:pseudo Newstonian linear analysis of isothermal and adiabatic inviscid slab thin disks
  - **Blondin & Shaw, 2007, ApJ 656, 366**: 2D simulations in conical thin disks around a neutron star

2. Steady Accretion Flows with a Shock

■ Set up

- **General relativistic inviscid flows in the Kerr space-time**
  - **The metric is constant in time.**
  - **The slef-gravity of the accreting matter is ignored.**
  - **The basic equations:**

$$(\rho_0 u^\alpha)_{;\alpha} = 0 \qquad T^{\alpha\beta}{}_{;\beta} = 0$$

- **The conical thin disk approximation is employed.**
  - **Only the equatorial plane is treated under the assumptions of** $u^\theta = 0$ **and** $\partial_\theta = 0$ **.**
- **The gamma–law EOS is used.**

$$P = (\gamma - 1)\rho_0 \varepsilon$$

Spherically Symmetric Accretion Flows

$$\partial_t = \partial_\theta = \partial_\phi = 0$$
$$u^\theta = u^\varphi = 0$$
$$r^2 \rho_0 u^r = const$$
$$h u_t = const$$

(*h*: enthalpy)

$$\frac{d}{dr} u^r = \frac{D_1}{D}$$

$$D = u_r u^r - b^2 (1 + u_r u^r)$$
$$D_1 = \frac{u^r}{r}\{2b^2(1+u^r u_r) - \frac{M}{r-2M}\}$$

b : sound velocity

$D = 0$ **critical point (= sonic point)**

$D_1 = 0$

regularity condition

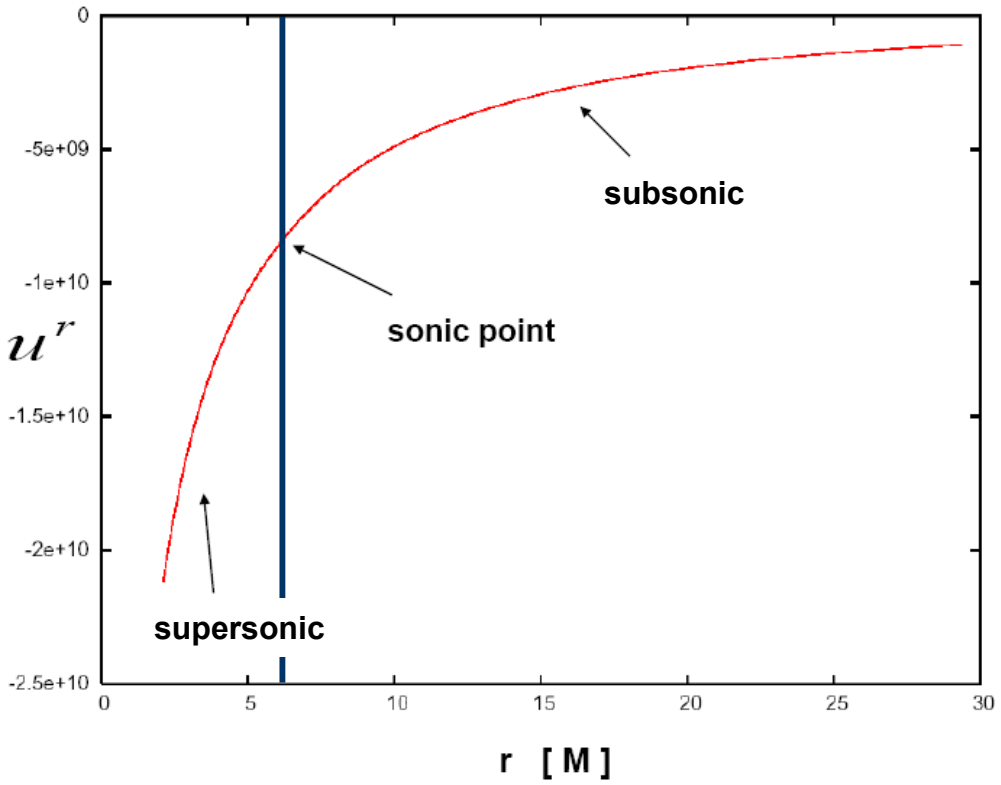

== Note ==

The accretion rate changes the density but does not affect the position of the sonic point.

Axisymmetric Accretion Flows in the Equatorial Plane

$$\partial_t = \partial_\theta = \partial_\phi = 0$$

$$u^\theta = 0$$

$$\theta = \frac{\pi}{2}$$

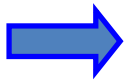

An ordinary differential equation similar to the previous equation.

$$\frac{du^r}{dr} = \frac{N}{D}$$

$$\begin{pmatrix} r^2 \rho_0 u^r = const & \text{Accretion rate} \\ -hu_t = const & \text{Bernoulli Constant} \\ -u_\phi / u_t = const & \text{Specific Angular Momentum} \end{pmatrix}$$

D = 0 : critical point (= sonic point)
N = 0 : regularity condition

$$D = u_r u^r - b^2(1 + u_r u^r)$$

$$N = \frac{2b^2 u^r}{r}(1 + u_r u^r) + \frac{1}{r^2(r^2 - 2Mr + a^2)}[(Mr^2 - a^2 r)u^r u_r u^r$$

$$+ (Mr^2 + Ma^2)u^r u_t u^t + Mau^r u^t u_\phi - (3Mar^2 + Ma^3)u^r u^\phi u_t$$

$$+ (r^3 - Ma^2 - 2Mr^2)u^r u^\phi u_\phi]$$

Multiple sonic points exist for some injection parameters.

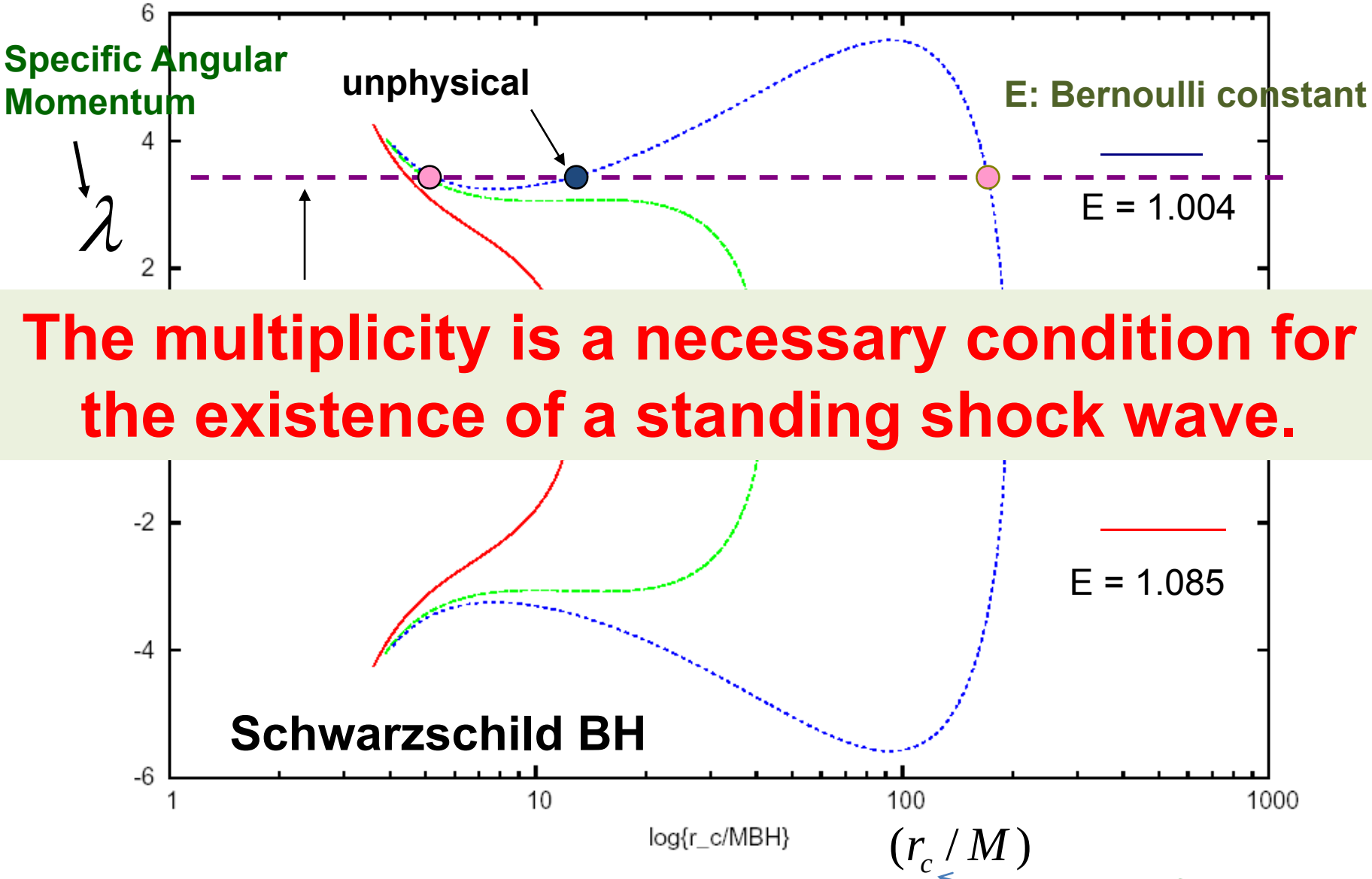

The multiplicity is a necessary condition for the existence of a standing shock wave.

A Schematic Profile of Shocked Accretion Flows to BH

※ **Post-shock flows are transonic for BH accretions.**

— **Adiabatic inviscid flows are supersonic at the event horizon.**

— **This is in sharp contrast to accretions onto neutron stars.**

※ **The specific angular momentum and Bernoulli constant are unchanged in passing through the shock wave.**

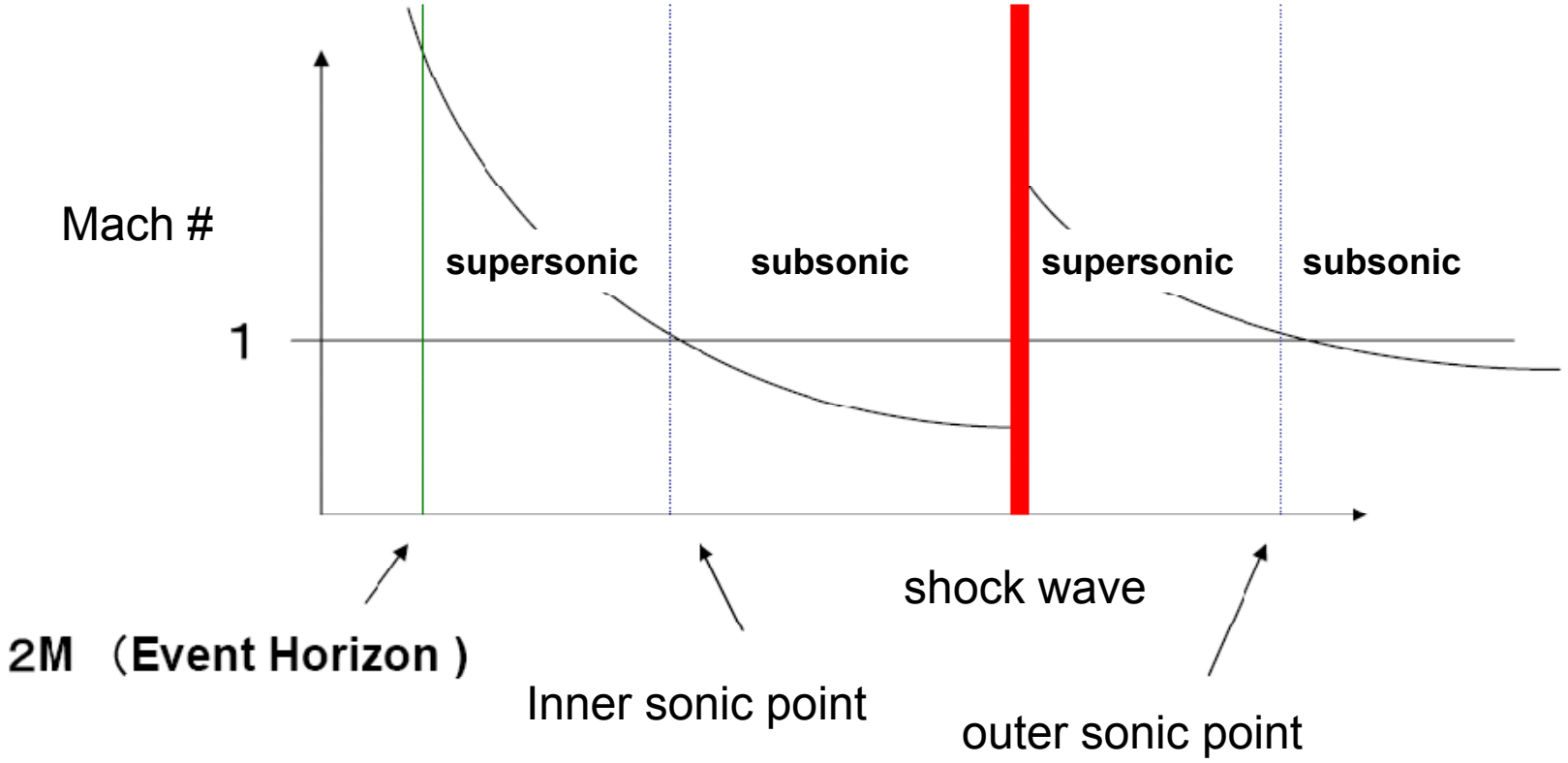

Two Possible Shock Positions

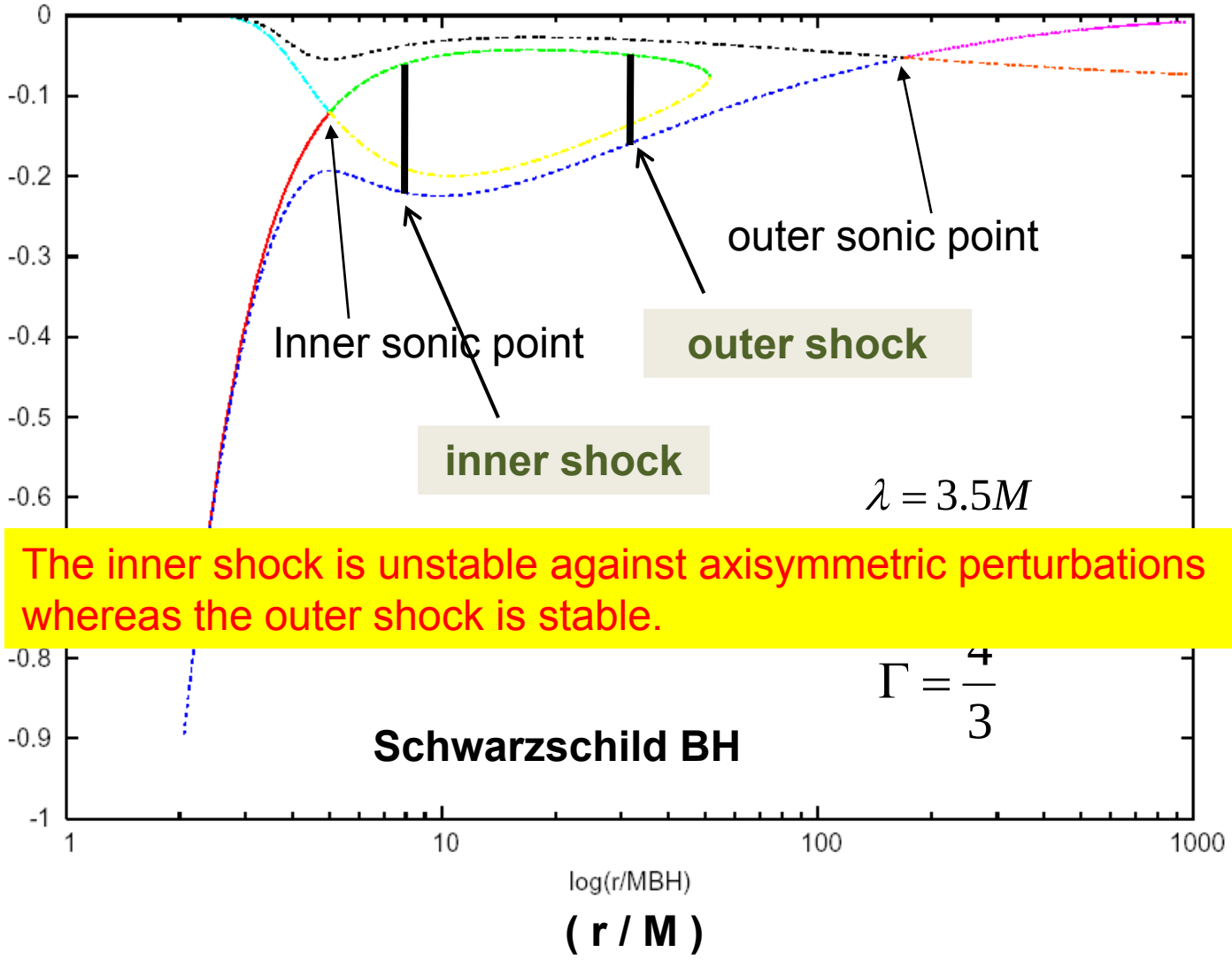

The inner shock is unstable against axisymmetric perturbations whereas the outer shock is stable.

Sonic Points as a Function of the Kerr Parameter

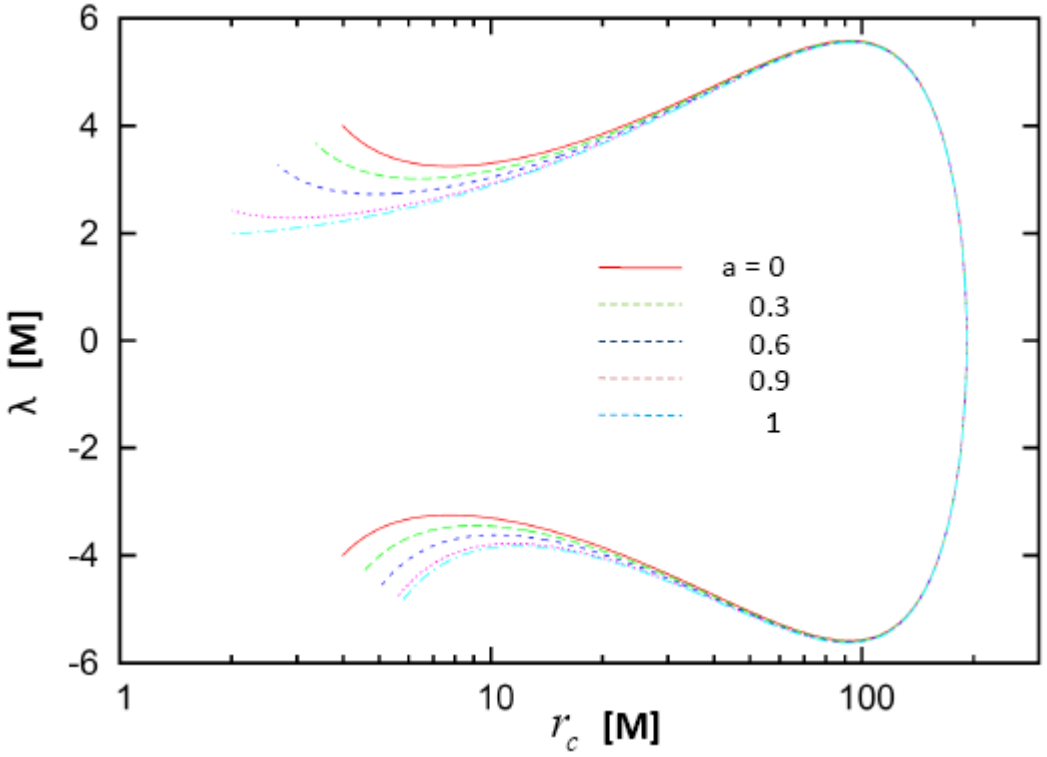

✓ The figure is not symmetric to the λ=0 line because of the BH rotation.

✓As the black hole rotates faster, the region of the injection parameters that allow the existence of multiple sonic points becomes narrower for λ>0 and wider for λ<0 owing to the frame dragging.

Injection Parameters for the Shock Existence

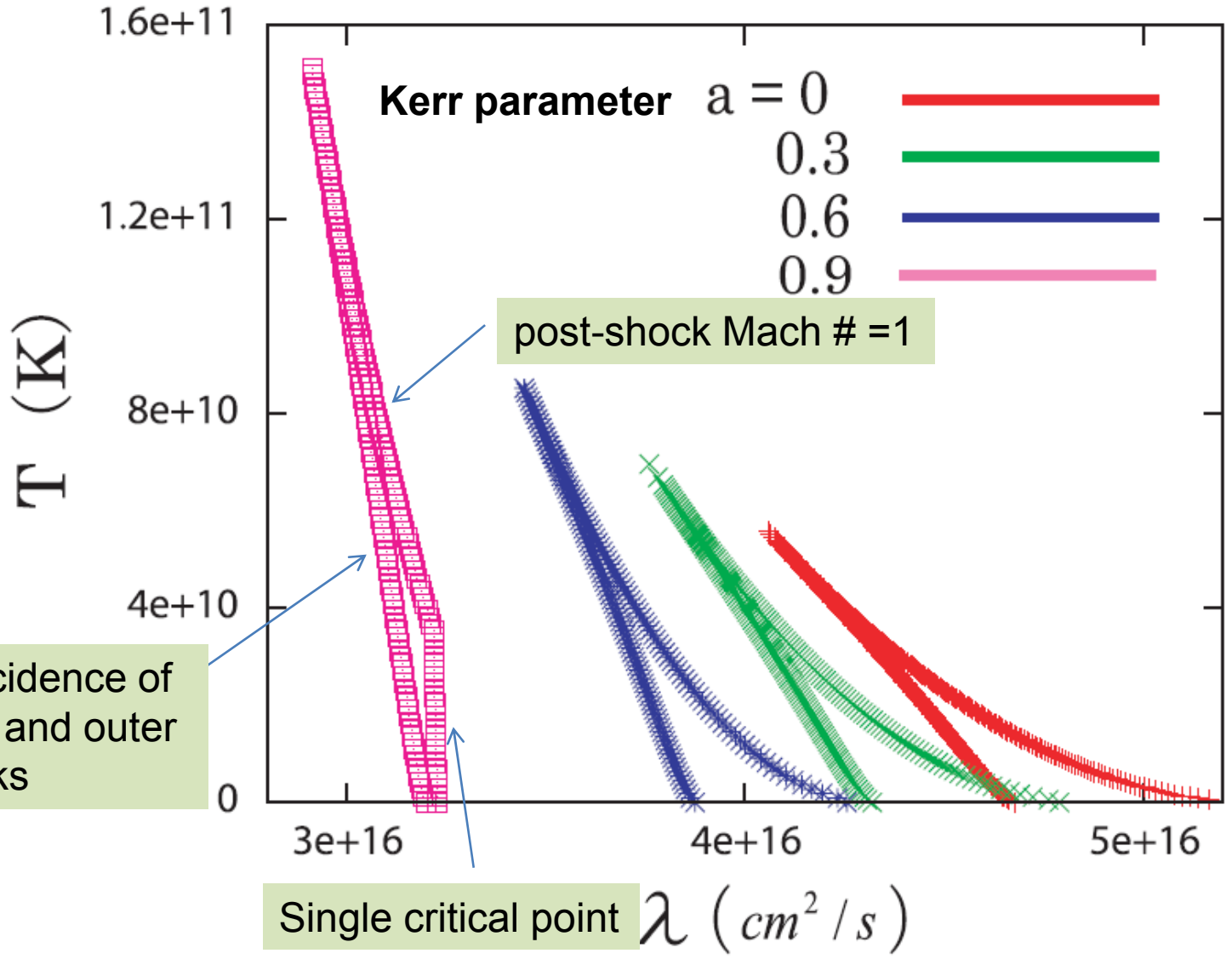

Difference between GR and Pseudo–Newtonian Approximation

$$\phi = -\frac{GM}{r - r_g}$$

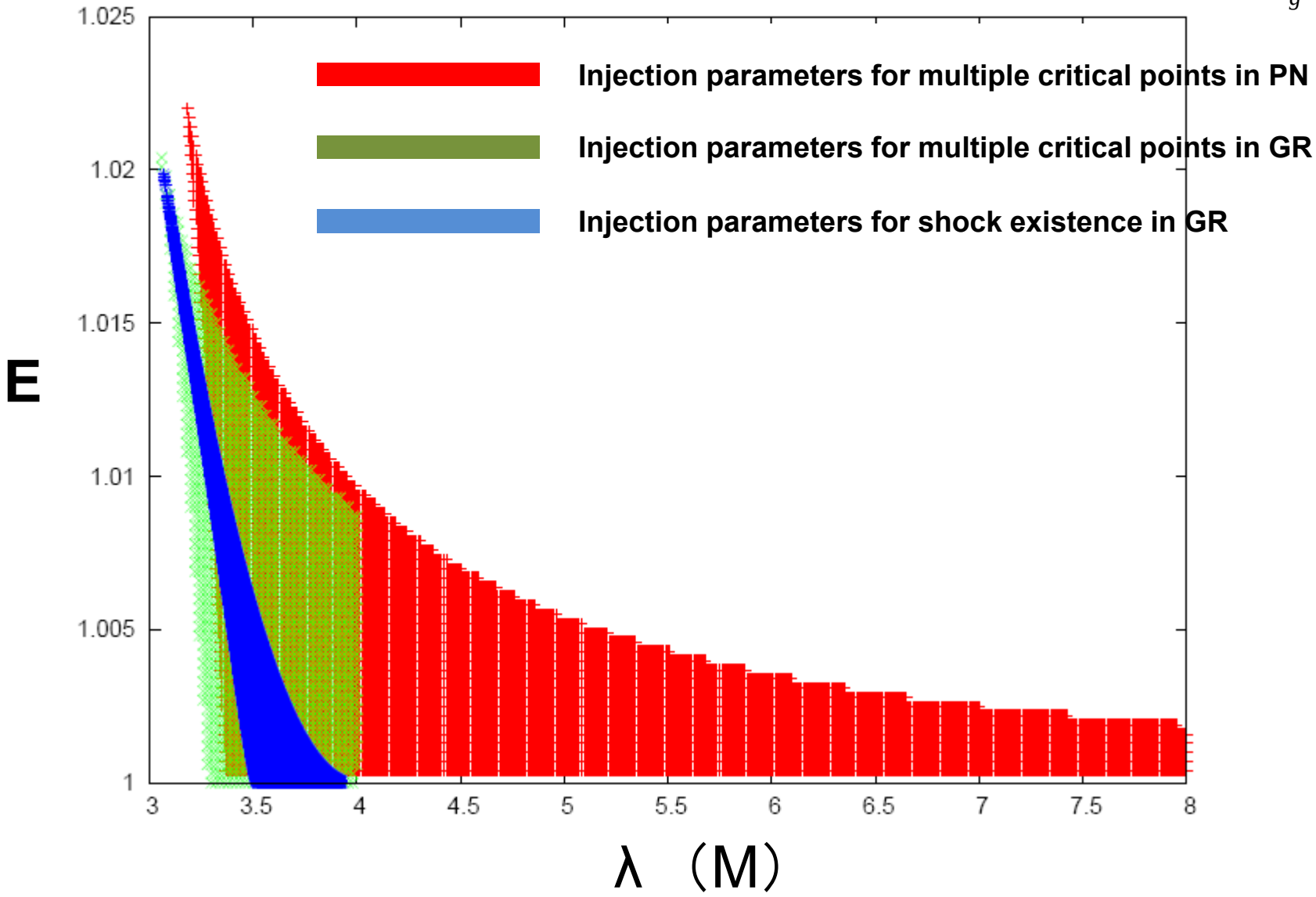

3. Linear Analysis

Linearized Equations

$$\begin{cases} Q = Q_{(0)} + Q_{(1)} \\ Q_{(1)}(t, r, \phi) = P(r)\exp\{-iwt + im\phi\} \end{cases}$$

$$\begin{cases} \partial_r f = \dfrac{i}{\rho_{0(0)}}\{\, \rho_{0(1)} u^{t(0)}\sigma + \rho_{0(0)}(\omega u^{t(1)} - m u^{\phi(1)})\,\} \\ \qquad\qquad f \equiv \dfrac{\rho_{0(1)}}{\rho_{0(0)}} + \dfrac{u^{r(1)}}{u_{r(0)}} \\ \partial_r q = \dfrac{i}{\rho_{0(0)} u^{r(0)} h_{(0)} u^{t(0)}}(\, \omega p_1 + \rho_{0(0)} u^{t(0)} h_{(0)} u_{t(0)} \sigma q\,) \\ \qquad\qquad q \equiv \dfrac{h_{(1)}}{h_{(0)}} + \dfrac{u_{t(1)}}{u_{t(0)}} \\ \partial_r V_{(1)} = i\dfrac{u^{t(0)}}{u^{r(0)}}\sigma V_{(1)} \\ \qquad\qquad V_{(1)} \equiv \omega(\, h_{(1)} u_{\phi(0)} + h_{(0)} u_{\phi(1)}\,) + m(\, h_{(1)} u_{t(0)} + h_{(0)} u_{t(1)}\,) \\ \partial_r S_{(1)} = i\dfrac{u^{t(0)}}{u^{r(0)}}\sigma S_{(1)} \\ \qquad\qquad \sigma \equiv \omega - m\dfrac{u^{\phi(0)}}{u^{t(0)}} \end{cases}$$

Instability Condition: Im *w* > 0

■ Boundary Conditions

- ➢ no perturbations in the pre-shock flows
- ➢ the Rankine-Hugoniot condition at the shock

$$\left[\, \rho_0 u^\mu \,\right] l_\mu = 0$$
$$\left[\, T^{\mu\nu} \,\right] l_\nu = 0$$

$l_\nu \equiv \psi_{,\nu}$: four vector normal to the shock surface

$\psi \equiv r - R_{sh}$

- ➢ **For unperturbed flows:** R_{sh} **= const.** $l_\mu = (0, 1, 0, 0)$
- ➢ **For perturbed flows:** $R_{sh} = R_{sh(0)} + \eta \exp(\, -i\omega t + im\phi \,)$

$$l_\nu = (i\omega\eta e^{-i\omega t + im\phi}, 1, 0, -im\eta e^{-i\omega t + im\phi})$$

- ➢ the regularity condition at the sonic point

Results

✓**The inner shock is unstable to the axisymmetric perturbation (*m*=0 mode) whereas the outer shock is stable.**

✓**The outer shock is unstable to some non-axisymmetric (*m*≠0 mode) perturbations.**

— **Some progressive modes (*m*>0) are unstable while all retrogressive modes (*m*<0) are stable.**

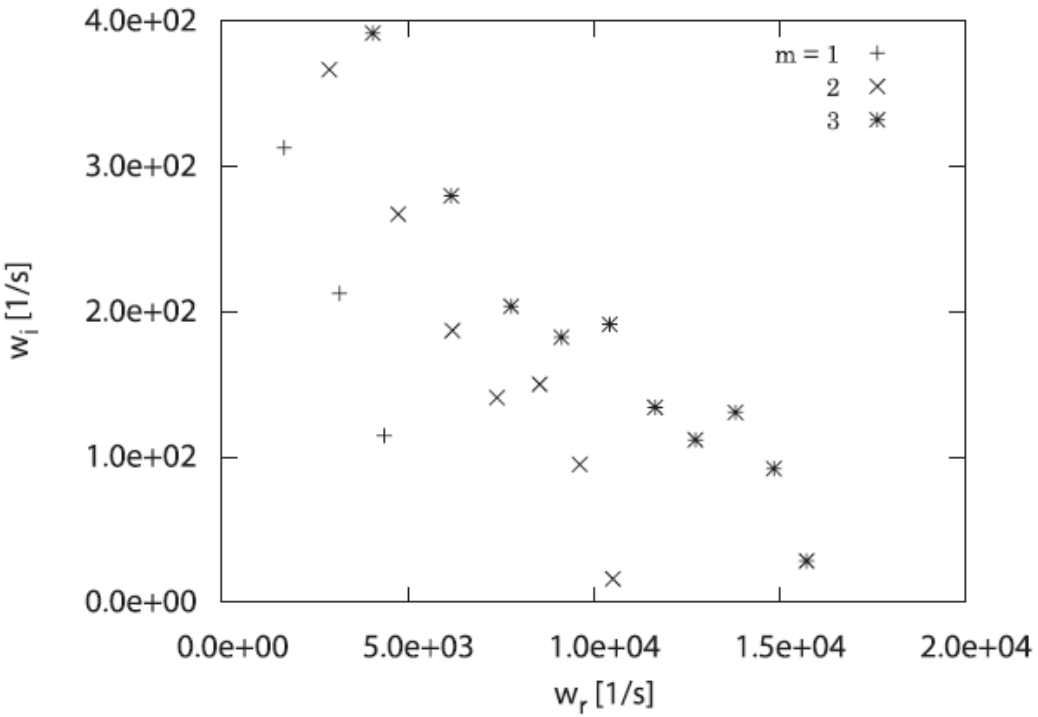

E **= 1.004**

$\lambda = 3.43 M_{BH}$

$\Gamma = 4/3$

The maximum growth rates for different mode sequences.

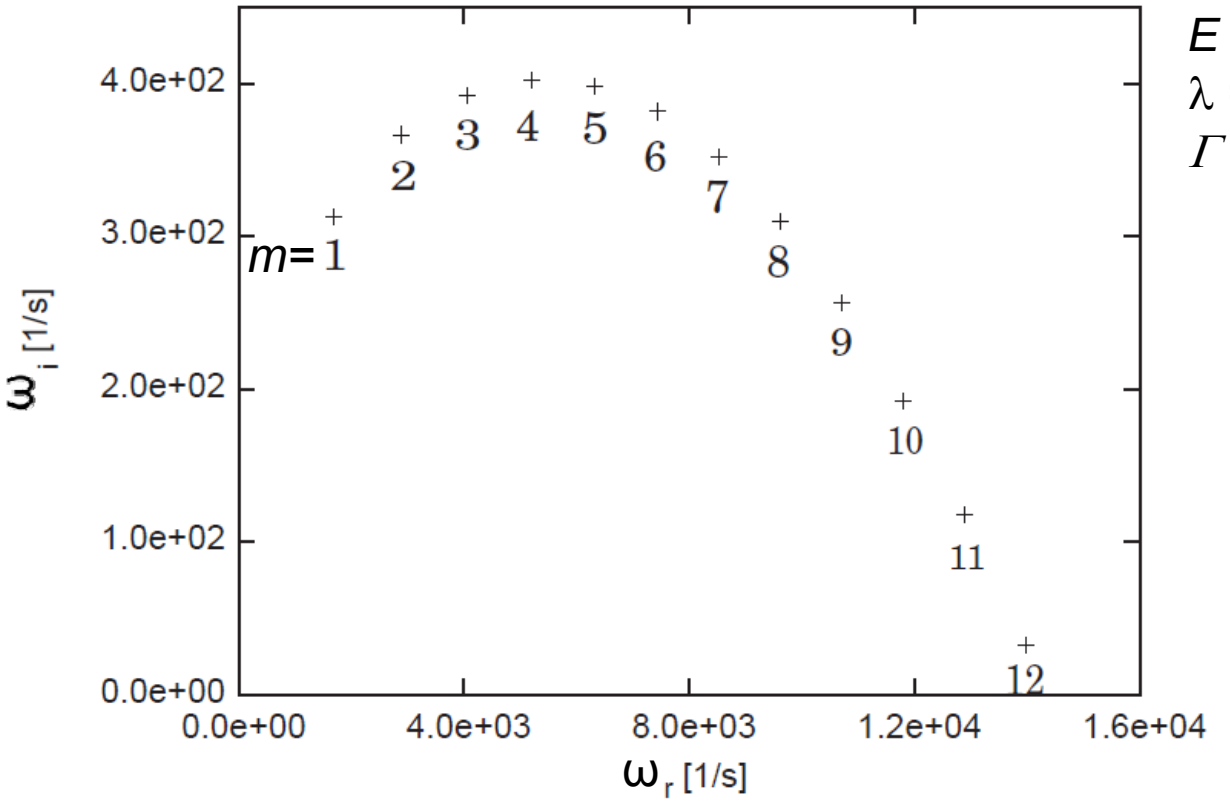

E = 1.004
$\lambda = 3.43 M_{BH}$
$\Gamma = 4/3$

Another Model

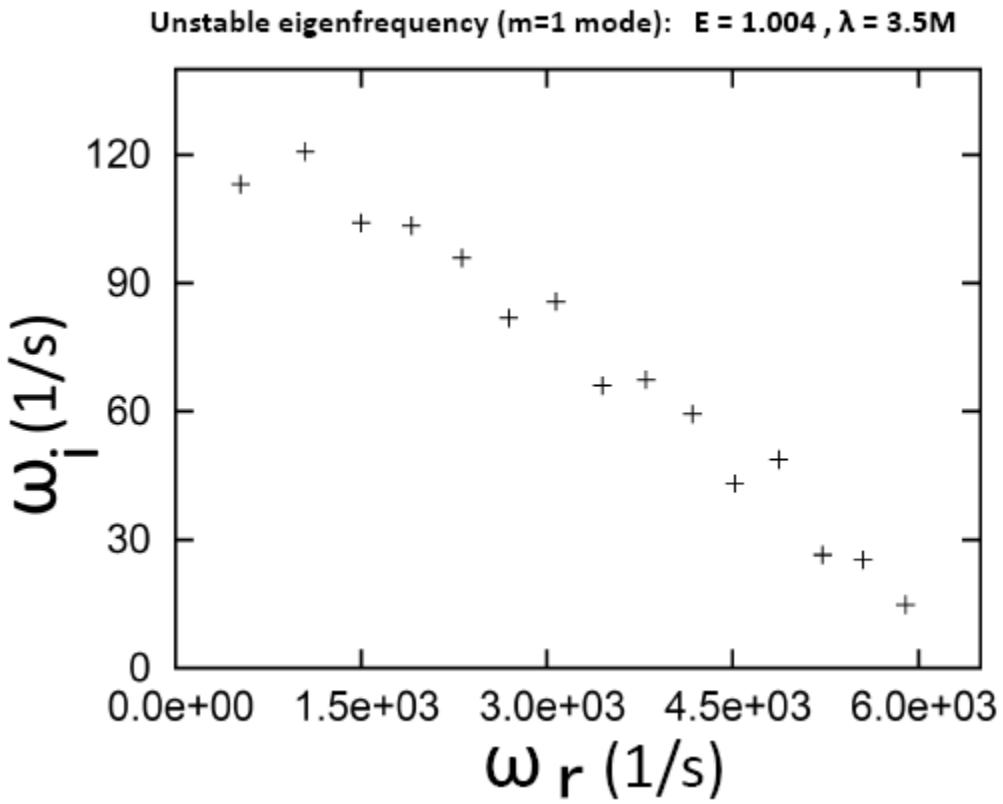

E = 1.004
$\lambda = 3.5M_{BH}$
$\Gamma = 4/3$

Instability Mechanism

The acoustic – acoustic cycle between the shock wave and corotation point has been suggested.

Gu & Foglizzo, 2003, A&A 409, 1
Gu & Lu, 2006, MNRAS 365, 647

※ Over-reflections at the corotation point are essential: Papaloizou – Pringle Instability

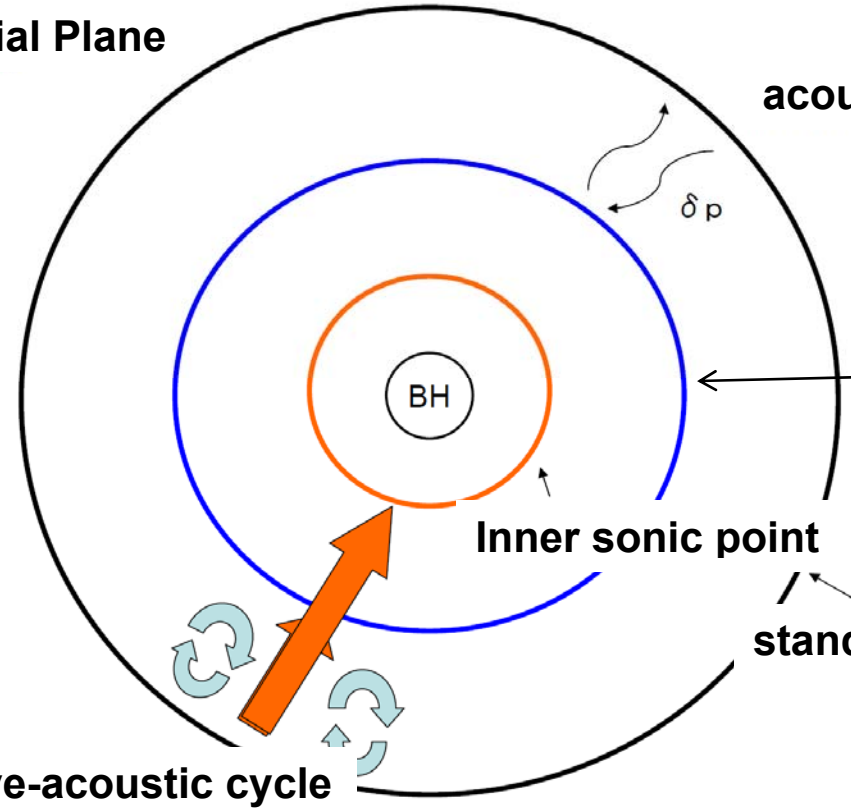

$$\omega_r - m\frac{u^r\left(r_{cor}\right)}{u^t\left(r_{cor}\right)} = 0$$

※ WKB approximation is not justified except for higher harmonics.

Corotation Points

$$\omega_r - m\frac{u^r\left(r_{cor}\right)}{u^t\left(r_{cor}\right)} = 0$$

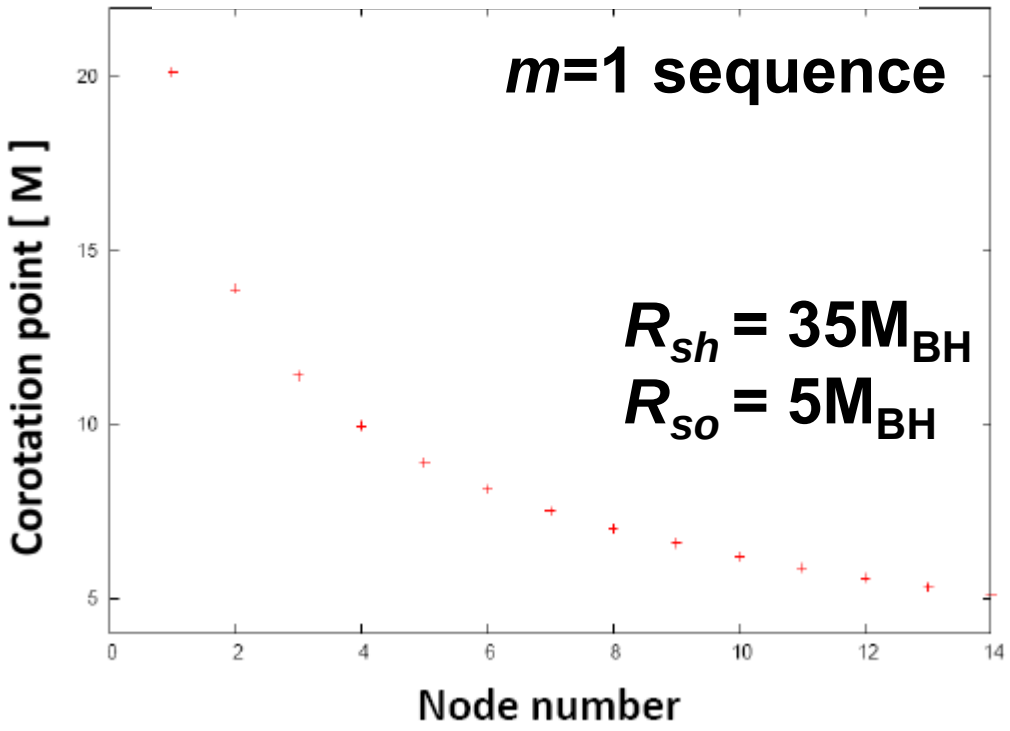

E **= 1.004**
λ = 3.5M_{BH}
Γ = 4/3

Comparisons of Cycle Frequencies:

The most unstable mode for each model

Shock-Corotation Point

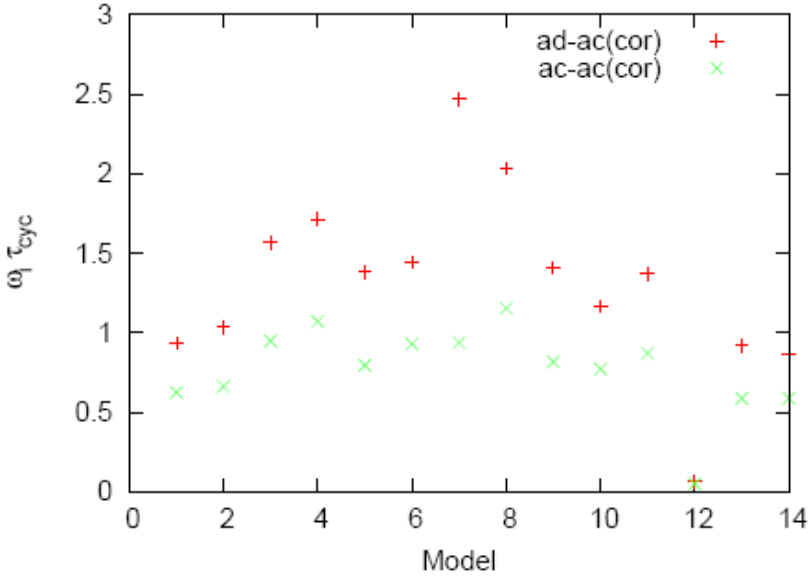

Shock-Inner Sonic Point

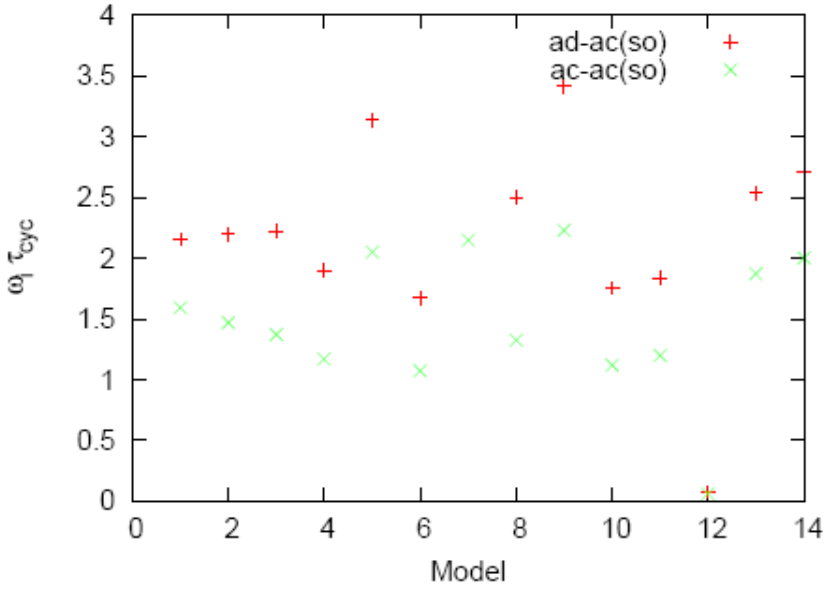

The results are consistent with those of Gu & Lu and support the acoustic-acoustic cycle between the shock and corotation point.

Comparisons of Cycle Frequencies:
m=1 mode sequence

E = 1.004
$\lambda = 3.5 M_{BH}$
Γ = 4/3

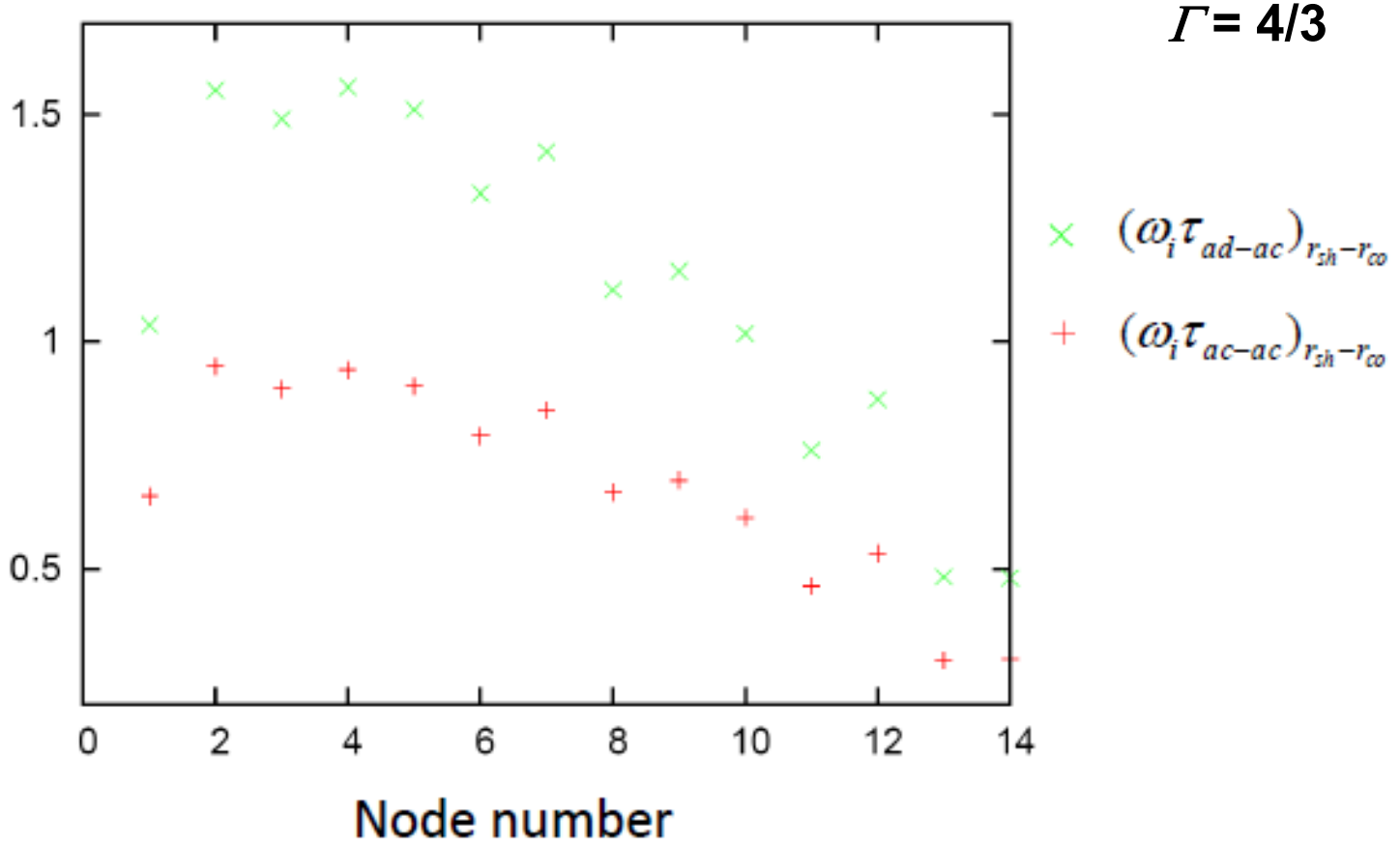

Dependence on the Kerr Parameter for Fixed Injection Parameters

$E = 1.004$
$\lambda = 3.5M_{BH}$
$\Gamma = 4/3$

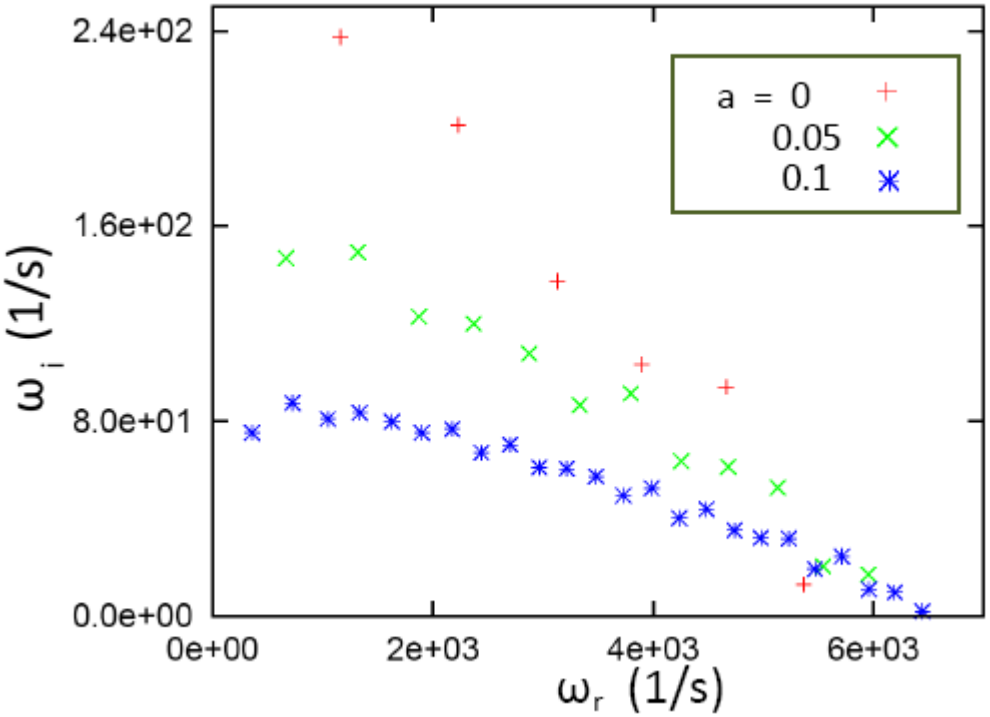

- ✓ As the Kerr parameter gets larger with the injection parameters being fixed, both the growth rates and the oscillation frequencies become smaller.
- ✓ This is mainly because the shock wave is located farther away.

Dependence on the Kerr Parameter for a Fixed Shock Radius

$E = 1.004$
$R_{sh} = 35M_{BH}$
$\Gamma = 4/3$

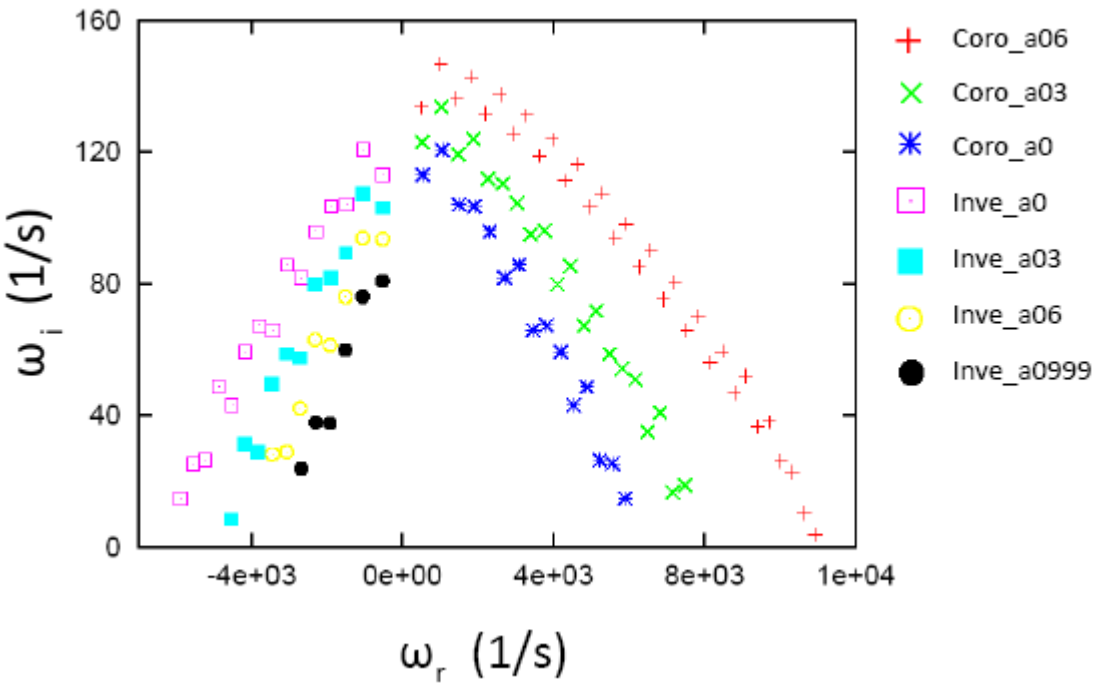

- ✓ As the Kerr parameter gets larger with the shock radius being fixed, the pre-shock Mach number becomes larger and, as a result, the growth rates becomes larger.
- ✓ The oscillation frequencies are affected very little.

4. Numerical Simulations of Nonlinear Evolutions

- ✓ **Multi-dimensional general relativistic hydrodynamical code based on the central scheme**
- ✓ **Kerr – schild coordinates employed to avoid the coordinatesingularity at the event horizon**
- ✓ **The eigen functions employed as an initial condition**
- ✓ **The black hole mass: $3M_{solar}$**
- ✓ **Computational domain: r ≲ 900km**
- ✓ **grid points:** $(r, \varphi) = (600, 60)$

Table 1. Initial Model Parameters

Model	Adiabatic Index Γ	Bernoulli Constant E	Specific angular momentum λ	inner sonic point r_{inso}	shock point r_{sh}	initial perturbed mode	amplitude
M1	$\frac{4}{3}$	1.004	3.43M	5.3M	16.1M	1	1 %
M2	$\frac{4}{3}$	1.004	3.46M	5.2M	23.2M	1	1 %
M3	$\frac{4}{3}$	1.004	3.50M	5.0M	34.8M	1	1 %
M4	$\frac{4}{3}$	1.004	3.56M	4.8M	78.4M	1	1 %
M5	$\frac{4}{3}$	1.001	3.50M	5.1M	16.9M	1	1 %
M6	$\frac{4}{3}$	1.005	3.50M	5.0M	50.2M	1	1 %
M7	$\frac{31}{30}$	1.13	3.80M	4.4M	38.7M	1	1 %
M8	$\frac{35}{30}$	1.02	3.70M	4.6M	64.2M	1	1 %
M9	$\frac{35}{30}$	1.02	3.60M	5.0M	14.0M	1	1 %
M10	$\frac{35}{30}$	1.03	3.60M	5.0M	32.4M	1	1 %
M11	$\frac{43}{30}$	1.001	3.35M	5.2M	40.6M	1	1 %
M12	$\frac{43}{30}$	1.004	3.15M	6.0M	36.5M	1	1 %
M1m2	$\frac{4}{3}$	1.004	3.43M	5.3M	16.1M	2	1 %
M1m3	$\frac{4}{3}$	1.004	3.43M	5.3M	16.1M	3	1 %
M1a10	$\frac{4}{3}$	1.004	3.43M	5.3M	16.1M	1	10 %
M1a100	$\frac{4}{3}$	1.004	3.43M	5.3M	16.1M	1	100 %

Results

M1モデル

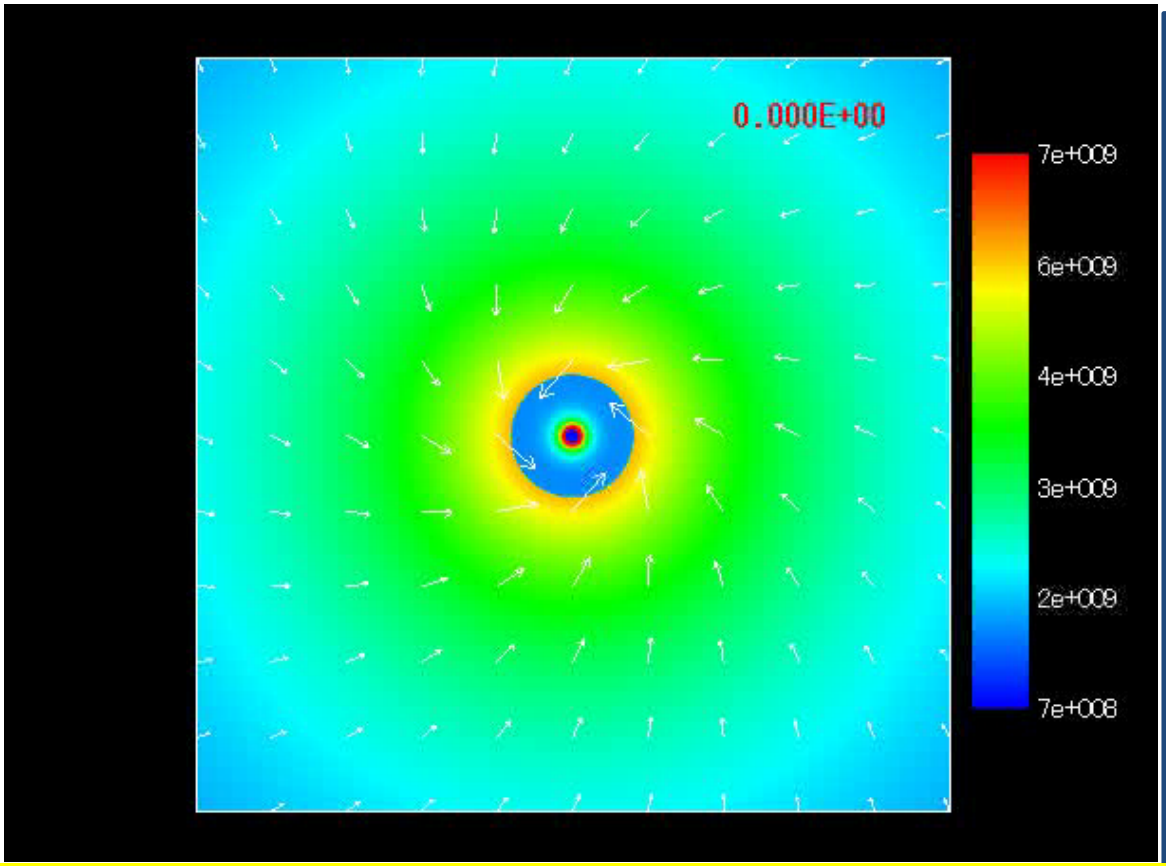

Unperturbed flow

Bernoulli constant

$E = 1.004$

specific angular momentum

$\lambda = 3.43M$

Inner sonic point $r_{so} = 5.3M$

shock $r_{shock} = 16.0M$

- ✓ **In the nonlinear phase, *m*=1 mode is dominant although it is not the most unstable mode in the linear phase, and a single spiral arm develops.**
- ✓ **The average shock radius (or the amplitude of *m*=0 mode) oscillates violently despite the mode is stable in the linear phase. The greater the pre-shock Mach number is, the larger the saturation amplitude becomes.**

Comparison with the Linear Analysis

The Fourier transform of the shock surface:

$$a_m(t) = \int_0^{2\pi} R_{sh}(\phi, t)\, e^{im\phi}\, d\phi,$$

The time evolution of *m*=1 mode.

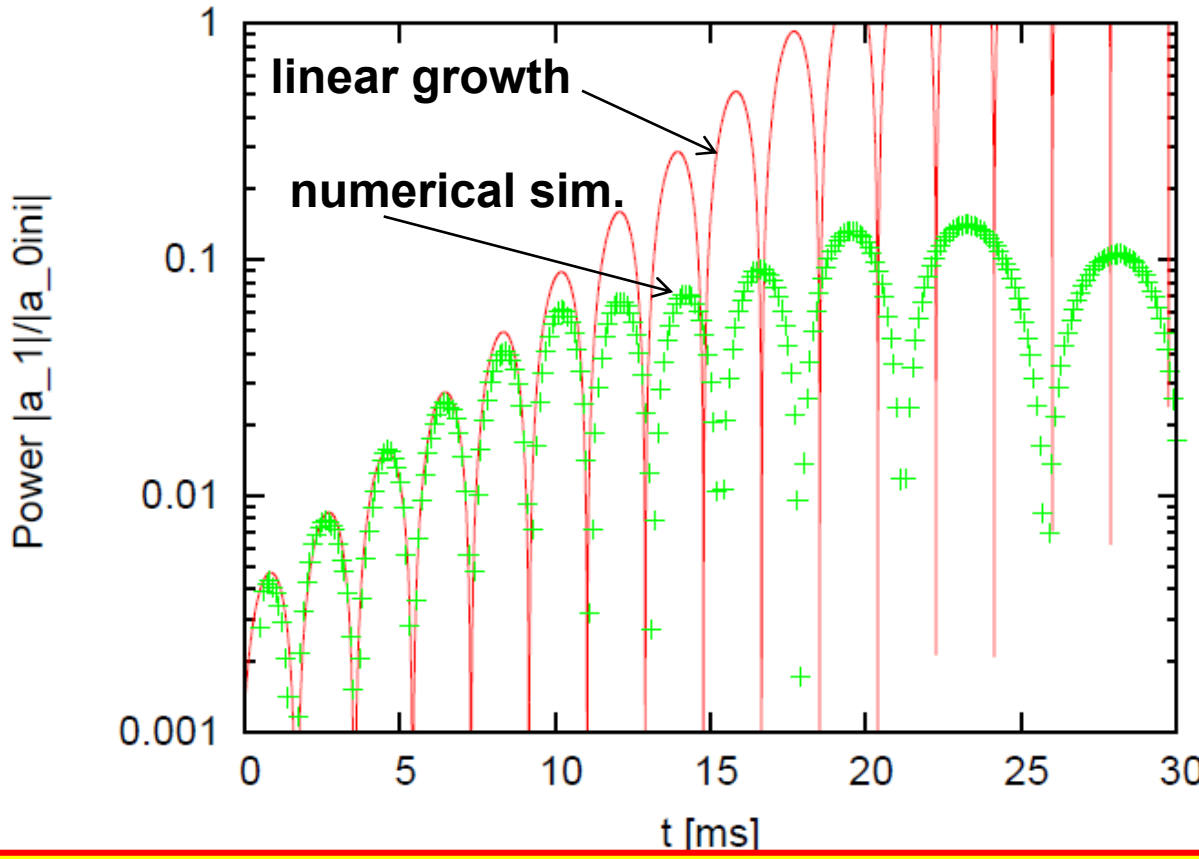

A good agreement is found until $|a_1/a_0|$ reaches ~10%, that is the saturation level.

Initial Perturbations and Mode Couplings

Initial perturbation : *m* = 2 mode

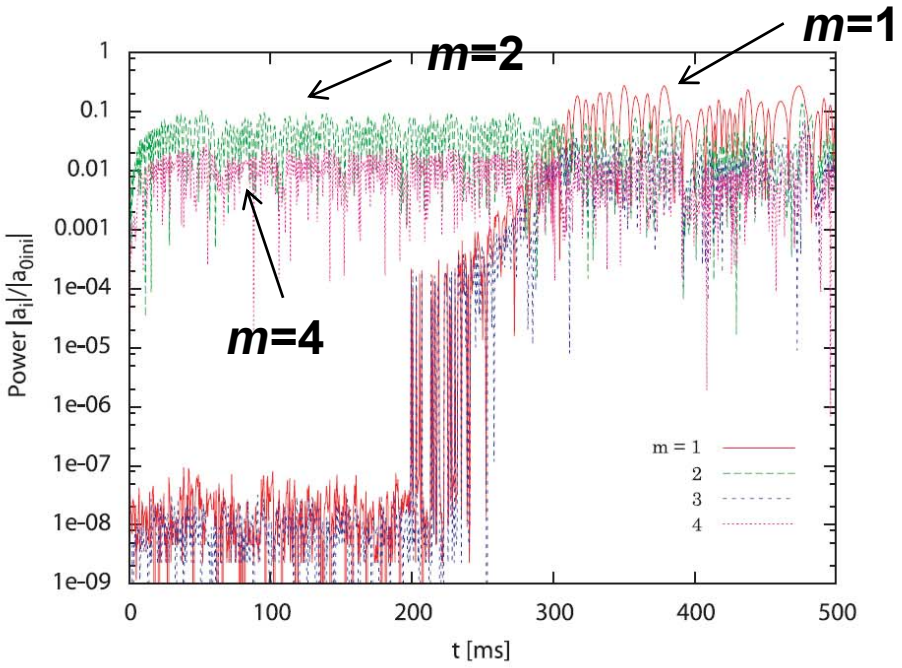

***m* = 3 mode**

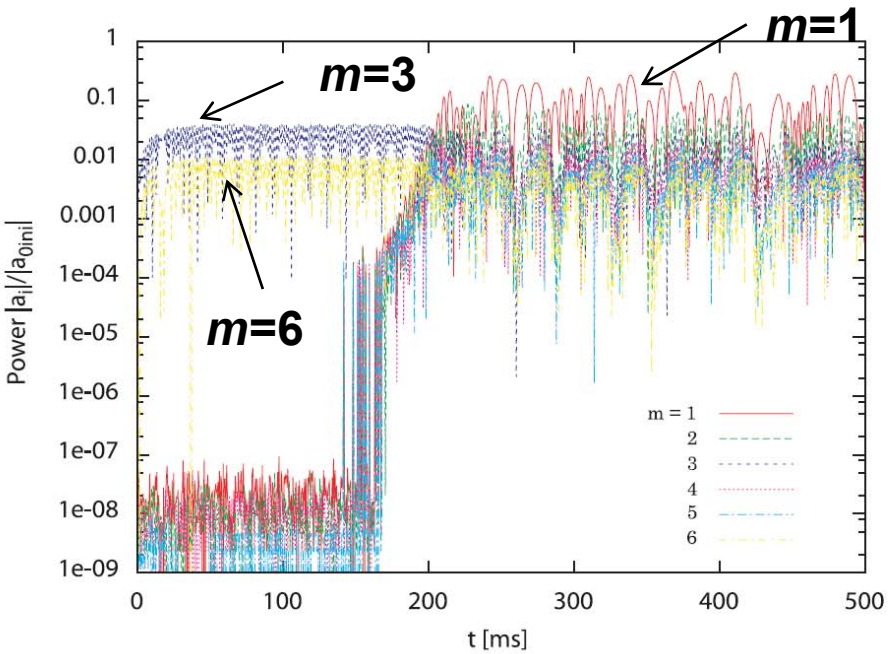

- ✓ **The mode couplings occur quadratically.**
- ✓ **After 200~300ms, all the modes are induced via numerical noises and m=1 mode becomes dominant irrespective of the initial perturbation mode.**

Induced Axisymmetric Oscillations

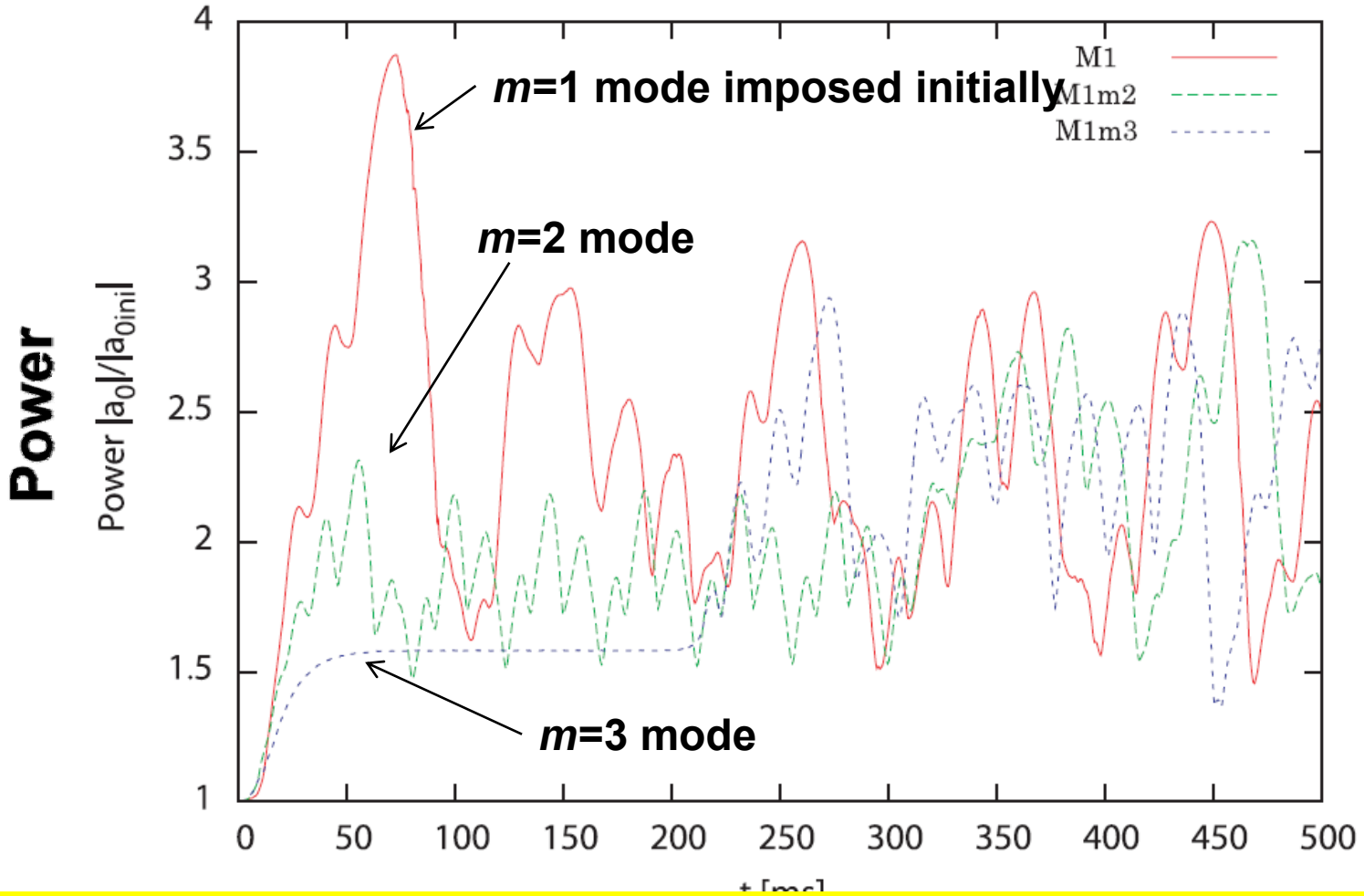

After ~250ms, when all the modes are produced, the amplitudes are almost identical among three cases.

Initial Perturbation Amplitudes

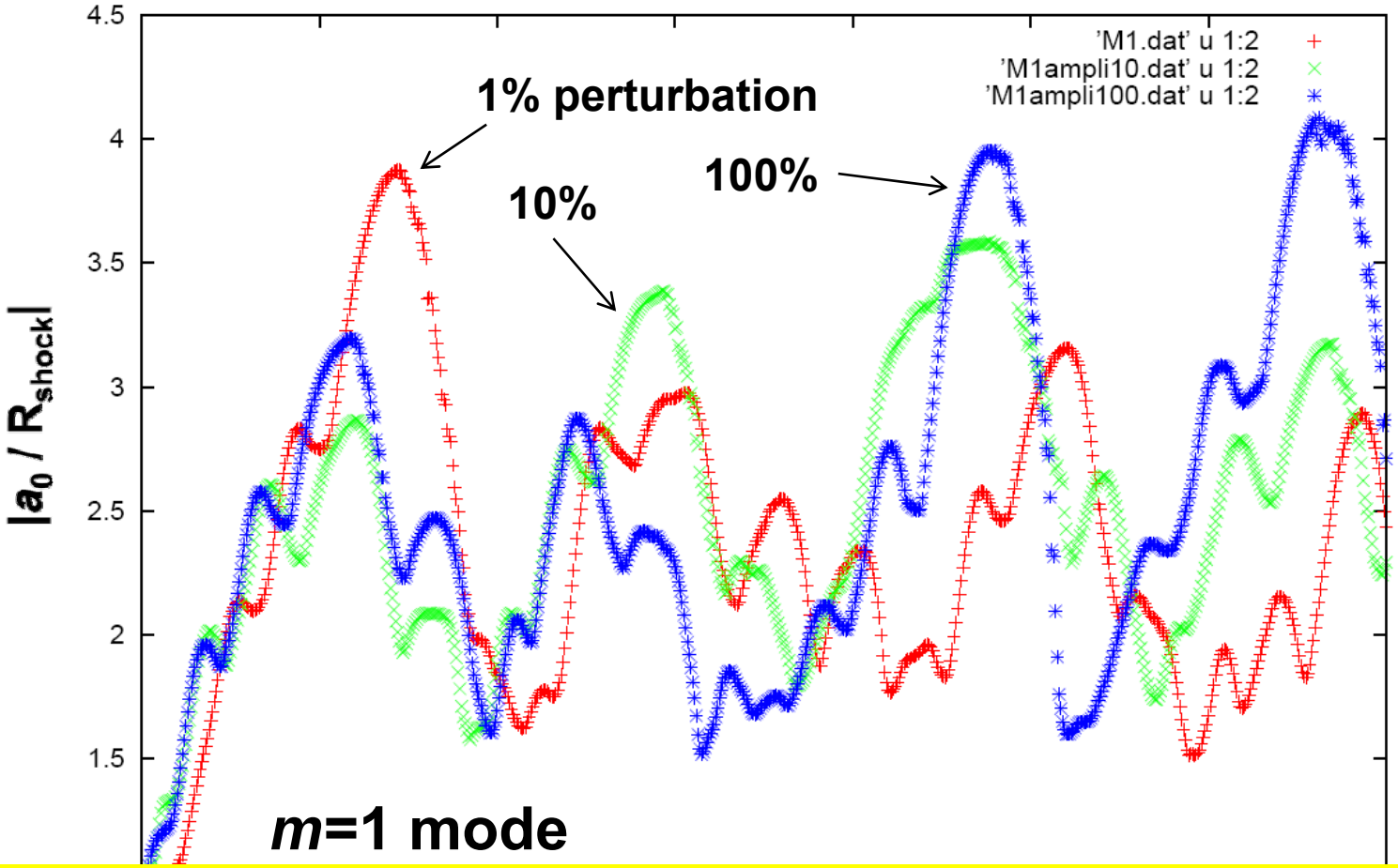

- ✓ The average shock radius oscillates with large amplitudes.
- ✓ Even 100% initial perturbation is saturated.
- ✓ The saturation level does not depend on the initial amplitude very much.

Kerr BHs

***a*=0.3**

M3モデル

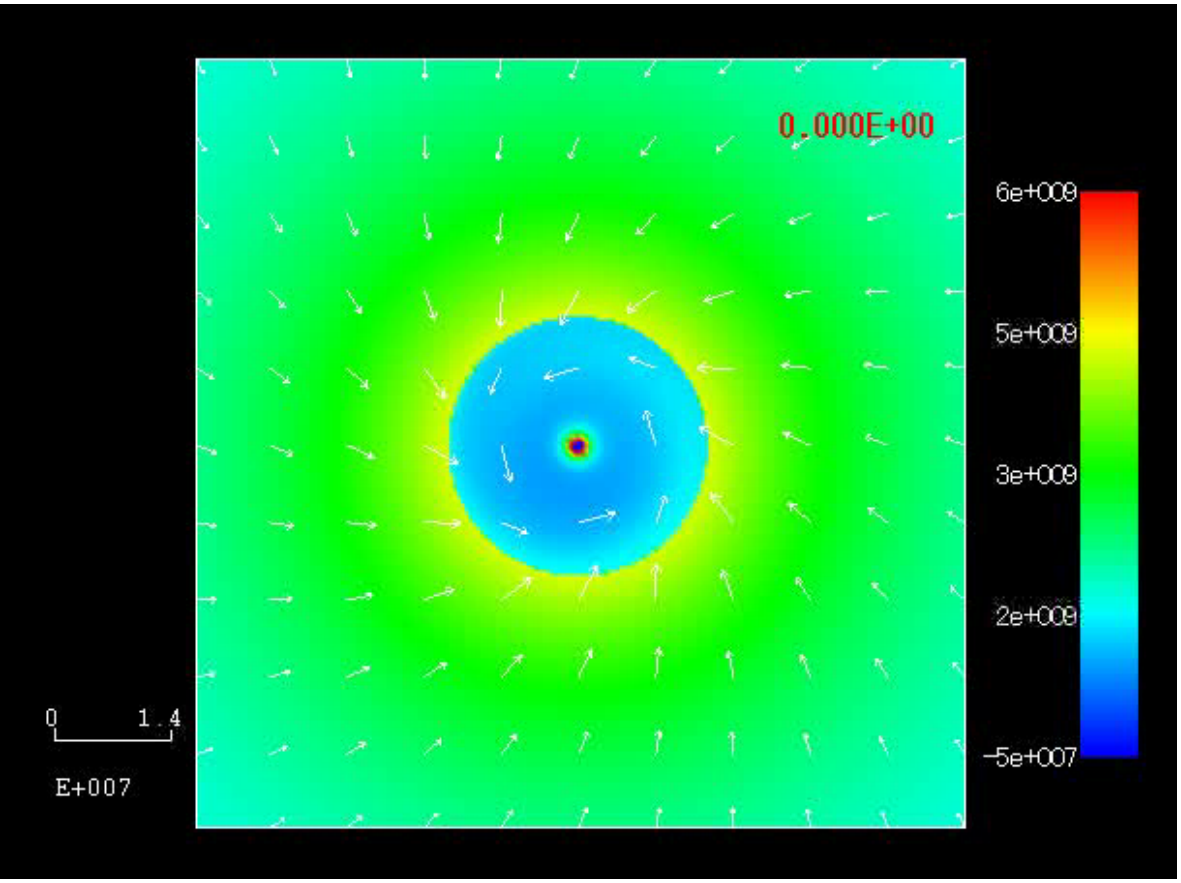

Unperturbed flow

Bernoulli constant

$E = 1.004$

Kerr parameters

a=0, ±0.3, −0.6, −0.999

Inner sonic point $r_{so} = 5M_{BH}$

shock $r_{shock} = 34.8M_{BH}$

color map : radial velocity

arrows : velocity vectors

initial perturbation

***m*=1 mode**

Amplitude : 1%

Comparison with the Linear Analysis

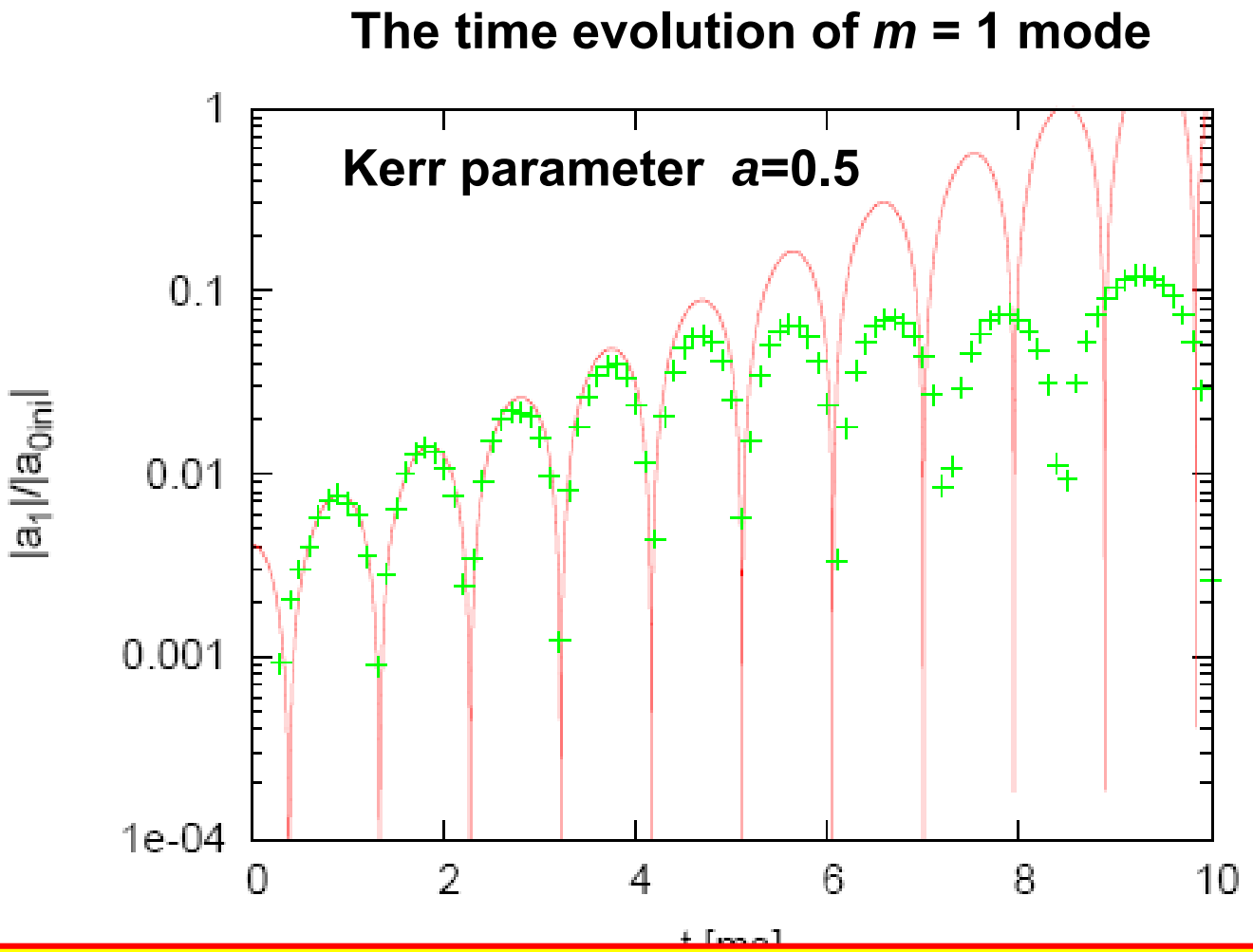

Again a good agreement is found until $|a_1/a_0|$ reaches the saturation level.

$a = 0$

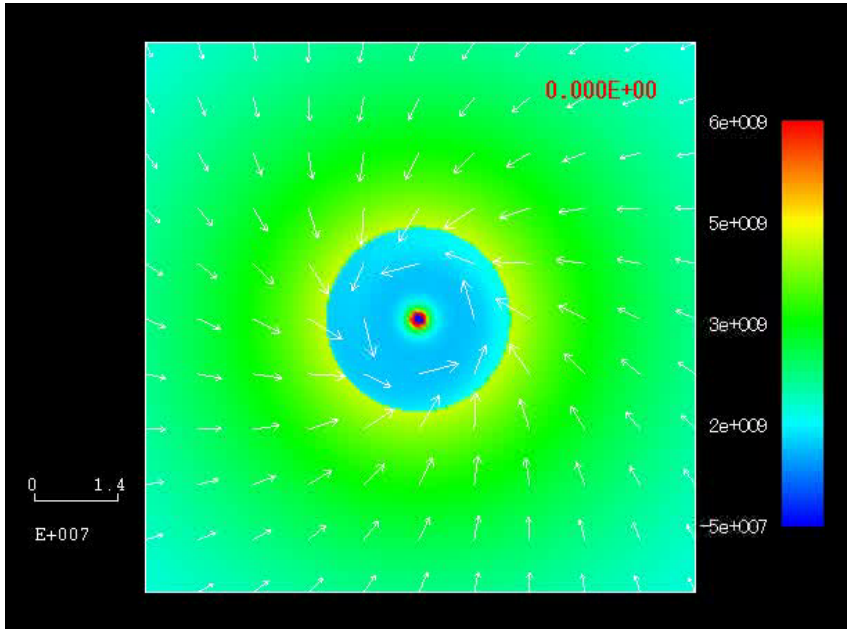

$a = 0.3$

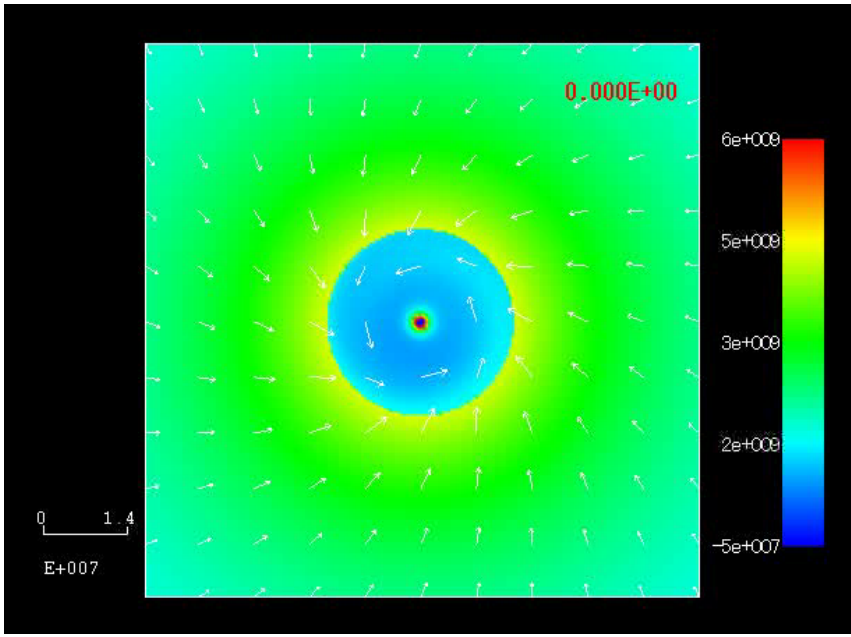

$a = -0.3$

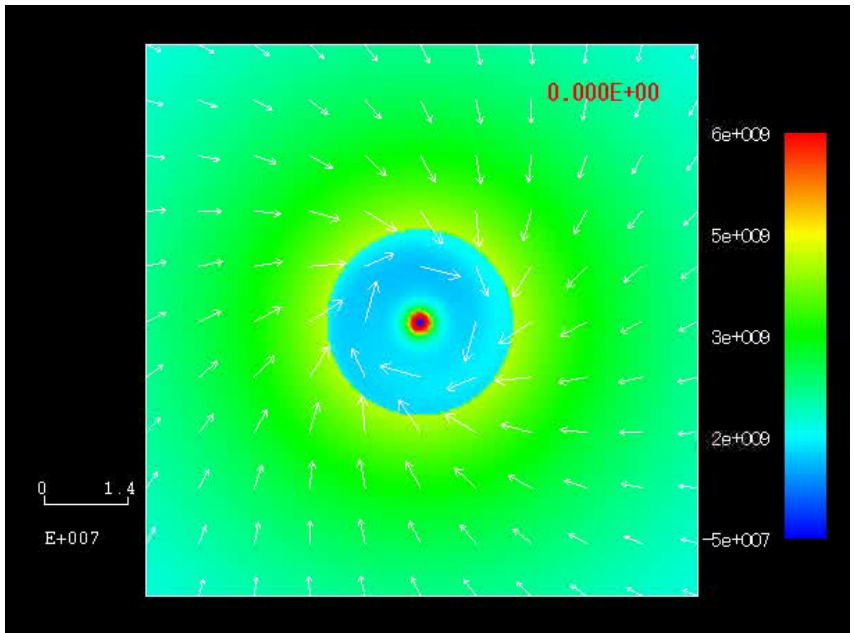

$a = -0.999$

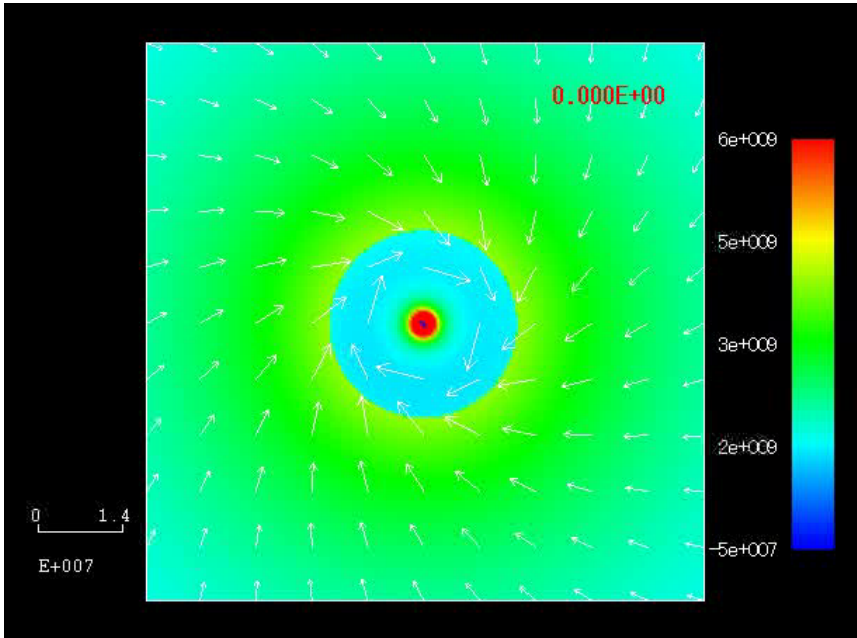

5. Astrophysical Implications

5.1 QPO (Quasi-Periodic-Oscillation) of BHs

- Quasi-periodic temporal var
  X / EUV / Optical radiations
  hole candidates.
- The observed periods are dif
  from object to object.
- Single objects have multiple
- The underlying mechanism r
  be revealed, but the QPOs pr
  reflect some activities of the
  disk near the BH.

Energy Spectrum of *m*=0 Mode

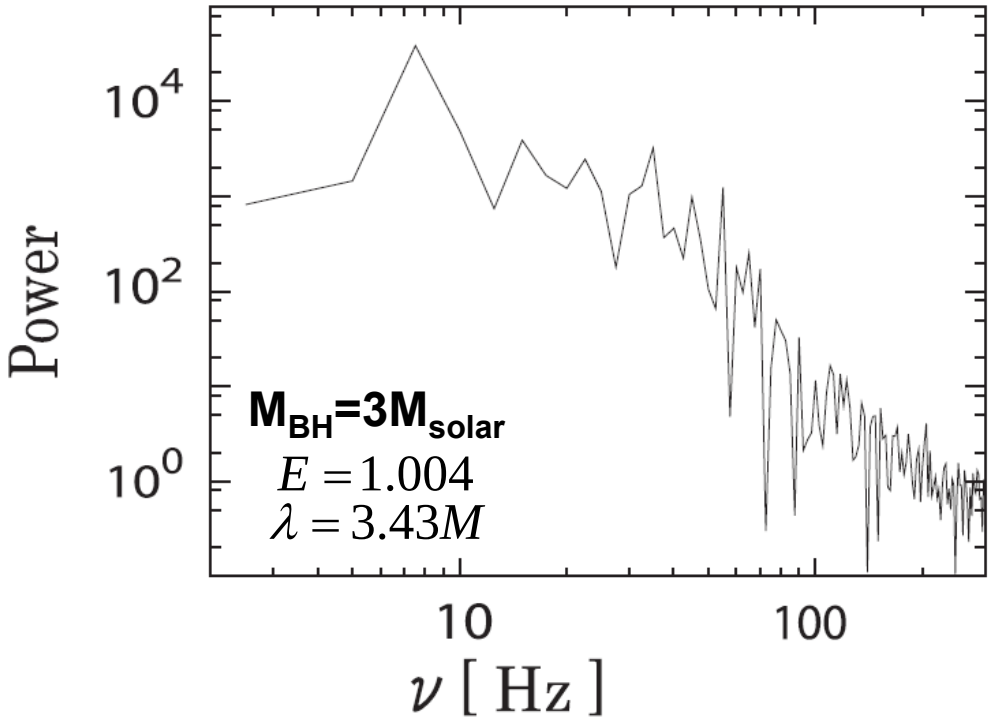

If the injection parameters of accretion flows from a companion are appropriate, the BH SASI may be a good candidate of a source for the BH QPOs of intermediate frequencies.

5.2 Massive Stellar Collapses with BH Formations

The Possibilty of Shock Existence:

- comparison with the rotating progenitor models by Heger et.al (2005)
- T = 0~1MeV, a = 0~1

$$\lambda = 6\times10^{16} \sim 10^{17}\,(\mathrm{cm}^2/\mathrm{s})$$

Evolution of angular momentum

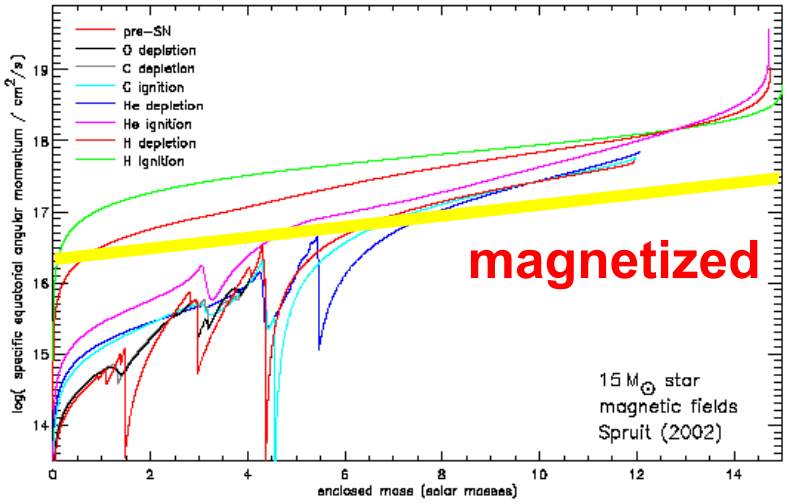

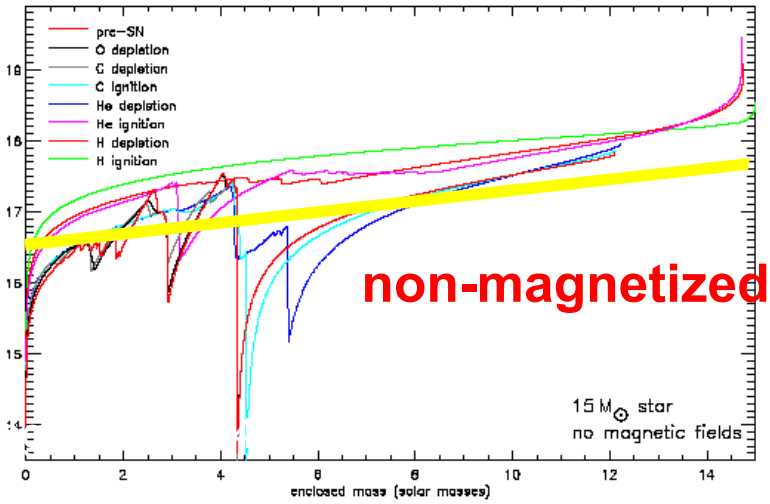

- ✓ **The range is rather narrow.**
- ✓ **SASI may occur as a short transient for magnetized, slowly rotating collapse.**
- ✓ **Centrifugally supported disks may inhibit the formation of shocked accretion flows for non-magnetized rapidly rotating collapse.**

Summary

- ✓ **We have done fully general relativistic linear and nonlinear analyses of the non-axisymmetric stability for the equatorial adiabatic inviscid accretions to a non-rotating and rotating black hole.**

- ✓ **We confirmed that the there are axisymmetric shocked accretion solutions for some injection parameters. GR treatment is necessary to determine the parameter region correctly. The frame dragging by rotating BHs tends to shift the region to lower angular momenta.**

- ✓ **It was also confirmed that the inner shock is unstable and the outer shock is stable against axisymmetric perturbations. Our numerical simulations demonstrated that the outer shock is quite robust to the perturbationns.**

- ✓ **The outer shock is unstable to the progressive ($m > 0$) non-axisymmetric perturbations. Low m modes are dominant in general in the linear phase and the dominance of $m = 1$ mode in the nonlinear phase leads to the formation of a single spiral arm in the accretion flow and oscillations of shock with large amplitudes.**

✓ **The numerical simulations are in good agreement with the linear analysis.**

✓ **Although the region of the injection parameters is not broad, the BH SASI may have important astrophysical implications for the BH QPOs and massive stellar collapses with a BH formation.**

Remaining issues are

- **The thickness (or the structure in the meridian section) should be taken into account.**
- **The effects of viscosity, cooling (or radiative transport) and magnetic fields should be investigated.**
- **Comparisons with more realistic models should be attempted.**